GEOPHYSICS, VOL. 60, NO. 6 (NOVEMBER-DECEMBER 1995); P. 1743–1749, 5 FIGS.

Seismic pore space compressibility and Gassmann's relation

Gary Mavko* and Tapan Mukerji*

ABSTRACT

The pore space compressibility of a rock provides a robust, model-independent descriptor of porosity and pore fluid effects on effective moduli. The pore space compressibility is also the direct physical link between the dry and fluid-saturated moduli, and is therefore the basis of Gassmann's equation for fluid substitution. For a fixed porosity, an increase in pore space compressibility increases the sensitivity of the modulus to fluid substitution. Two simple techniques, based on pore compressibility, are presented for graphically applying Gassmann's relation for fluid substitution. In the first method, the pore compressibility is simply reweighted with a factor that depends only on the ratio of fluid to mineral bulk modulus. In the second technique, the rock moduli are rescaled using the Reuss average, which again depends only on the fluid and mineral moduli.

INTRODUCTION

Seismic, mechanical, and reservoir properties of rocks are determined, in part, by pore space compressibility. Pore compressibility controls production-related formation compaction, surface subsidence, and stress redistributions. It impacts the generation of overpressure from phase changes, such as dehydration reactions and hydrocarbon maturation (Bredehoeft and Hanshaw, 1968; Jizba, 1991). It is also a key factor affecting fluid diffusivities in reservoirs.

Fortunately, pore compressibility is also a key parameter controling seismic wave propagation, which is the basis of sonic logging and 3-D seismic reservoir imaging. Increasing pore compressibility decreases seismic velocity. It also enhances the sensitivity of seismic velocities to changes in pore fluid type, pore pressure, stress, and saturation, and therefore provides the basis for geophysical monitoring of reservoir production and enhanced oil recovery (EOR) processes (Nur, 1989).

In this paper, we focus on the seismic velocity signature of pore space compressibility. We show, first, how pore compressibility can be estimated directly from measured seismic velocities. Next, we show how the pore compressibility is the link between velocities in dry and fluid-saturated rocks, which is the physical basis of Gassmann's (1951) equation for fluid substitution. Finally, we introduce simple techniques for applying Gassmann's relation graphically, for any mineralogy and any pore fluid type, from a single set of curves.

DRY ROCK COMPRESSIBILITY

Consider a rock as a linear elastic mineral frame containing a pore space of arbitrary pore volume and geometric complexity. Using the Betti-Rayleigh reciprocity theorem (see Appendix), we can write the dry rock compressibility at constant pore pressure, β_{dry}, which is the reciprocal of dry rock bulk modulus, $K_{dry} = \beta_{dry}^{-1}$, as (Walsh, 1965; Zimmerman, 1991)

$$\frac{1}{K_{dry}} = \frac{1}{K_0} + \frac{\phi}{K_\phi}, \tag{1}$$

where

$$\frac{1}{K_\phi} = \frac{1}{v_p}\left.\frac{\partial v_p}{\partial \sigma}\right|_P. \tag{2}$$

Here K_0 is the mineral bulk modulus, and ϕ is the porosity, defined as the volume of pore space divided by the total volume. K_ϕ^{-1} is the effective dry rock pore space compressibility, defined as the ratio of the fractional change in pore volume v_p to an increment of applied external hydrostatic stress σ at *constant pore pressure*. Note that K_ϕ^{-1} is *not* the compressibility of the fluid in the pores. We will also refer to K_ϕ as the "pore space stiffness." This is easily related to another pore compressibility, $K_{\phi P}^{-1}$, that is more familiar to reservoir engineers and hydrogeologists:

Manuscript received by the Editor April 11, 1994; revised manuscript received April 19, 1995.
*Rock Physics Laboratory, Dept. of Geophysics, Stanford University, Stanford, CA 94305-2215.

$$\frac{1}{K_{\phi P}} = -\frac{1}{v_p}\left.\frac{\partial v_p}{\partial P}\right|_{\sigma}, \tag{3}$$

which is the ratio of the fractional change in pore volume to an increment of applied pore pressure at constant confining pressure, by (Zimmerman, 1991)

$$\frac{1}{K_{\phi p}} = \frac{1}{K_\phi} - \frac{1}{K_0}. \tag{4}$$

Equation (1) states that the effective compressibility of the rock is equal to the compressibility of the mineral grains, plus an additional compressibility because of the pore space. It assumes that inelastic effects in the dry frame, such as viscosity and friction, can be ignored (generally a good assumption for the small strains induced by seismic waves), that the seismic wavelength is much longer than the scale of the grains and pores, and that the mineral material in the frame has homogeneous stiffness. Although the latter is not strictly true, the differences among the moduli of various minerals are generally much smaller than the difference between the moduli of the mineral and pore fluid. Hence, it is usually adequate to use an average mineral modulus for K_0. Both assumptions are common to most effective media models of porous rocks (Gassmann, 1951; Biot, 1956; Eshelby, 1957; Walsh, 1965; O'Connell and Budiansky, 1974; Kuster and Toksöz, 1974). It is important to note that equation (1) is a rigorous result and not simply a heuristically derived harmonic average of minerals and pores. Furthermore, it should not be confused with the Reuss (1929) average of minerals and pores, which has a similar appearance.

Equation (1) is otherwise quite general. It applies to any porosity and to any pore geometry. A very powerful result, therefore, is that pore space compressibility can be estimated directly from seismic velocities (assuming that K_0 and ϕ are known), since

$$K_{dry} = \rho\left(V_P^2 - \frac{4}{3}V_S^2\right), \tag{5}$$

where ρ is the bulk density, and V_P and V_S are the seismic compressional and shear wave velocities, respectively.

Figure 1 shows a plot of normalized dry bulk modulus, K_{dry}/K_0, versus porosity, computed from equation (1) for various values of normalized pore space stiffness, K_ϕ/K_0. Also shown, for reference, are the Voigt (1928) $K_{dry}^{(V)}$ and Reuss (1929) $K_{dry}^{(R)}$ upper and lower bounds on dry rock modulus

$$\begin{aligned} K_{(dry)}^{(V)} &= K_0(1-\phi) + K_{air}\phi \approx K_0(1-\phi), \\ K_{dry}^{(R)} &= ((1-\phi)/K_0 + \phi/K_{air})^{-1} \approx 0, \end{aligned} \tag{6}$$

where K_{air} is the bulk modulus of the pore-filling gas, which is taken here to be zero. It is important to emphasize that in this discussion K_{dry} is the rock modulus at constant pore pressure. This is the case when the bulk modulus of the pore fluid is negligible compared with the mineral bulk modulus, as for example air at room conditions. One should be cautious that a hydrocarbon gas at high in-situ pressures can have a *nonnegligible* bulk modulus, and must be treated as a "saturating fluid" as discussed in the next section.

These two bounds bracket the range of possible dry rock moduli in terms of the properties of the two end-member phases (in this case mineral and infinitely compressible gas). K_{dry} will always lie between $K_{dry}^{(V)}$, and $K_{dry}^{(R)}$. (The same thing can be said for the Hashin-Shtrikman (1963) bounds, which are narrower than the Voigt-Reuss bounds.) As seen from the contours in Figure 1, the position of K_{dry} relative to the bounds is an indication of pore stiffness: stiffer pores, with $K_\phi \approx (0.3 \text{ to } 0.5)K_0$, put K_{dry} closer to the upper bound, while softer pores, with $K_\phi \approx (0.0 \text{ to } 0.1)K_0$, put K_{dry} closer to the lower bound. Materials with moduli on the Reuss bound behave like suspensions, with no intrinsic pore stiffness, $K_\phi = 0$.

The data points plotted in Figure 1 are dynamic bulk moduli (calculated from ultrasonic velocities) for (1) 10 clean sandstones, all at a pressure of 40 MPa (Han, 1986), (2) a single clean sandstone at pressures ranging from 5 to 40 MPa (Han, 1986), and (3) porous glass (Walsh et al., 1965). Effective pore space compressibilities for each point can be read directly from the contours. The 10 clean sandstones (solid triangles) show that as the porosity decreases (which could be caused by the addition of cement) the pore space stiffness generally increases, in this case from $K_\phi/K_0 \approx 0.16$ at $\phi \approx 0.2$ to $K_\phi/K_0 \approx 0.22$ at $\phi \approx 0.1$. The single sandstone at variable pressure (open triangles) shows the expected result that pore space stiffness increases with confining pressure, approximately doubling from $K_\phi/K_0 \approx 0.07$ at 5 MPa to $K_\phi/K_0 \approx 0.14$ at 40 MPa. This type of increase has been alternately interpreted as the sequential closing of cracks with different aspect ratios (Walsh, 1965; Kuster and Toksöz, 1974), the closing and shortening of

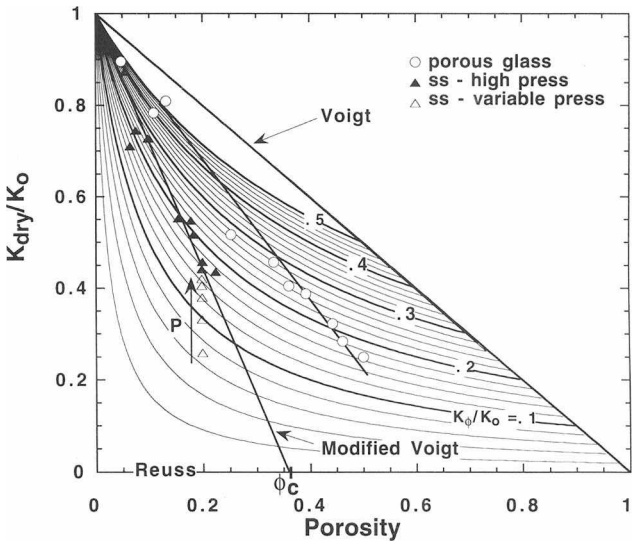

FIG. 1. Normalized dry rock bulk modulus versus porosity with contours of constant pore space stiffness labeled. Open circles show moduli data for glass foam (Walsh et al., 1965); closed triangles are for ten clean sandstones at 40 MPa confining pressure (Han, 1986); open triangles are for a single clean sandstone at confining pressures of 5, 10, 20, 30, and 40 MPa (Han, 1986). Arrow shows direction of increasing pressure.

tapered crack tips (Mavko and Nur, 1978), or the decreasing compliance of Hertzian grain contacts (Murphy et al., 1993). Regardless of ambiguities of these interpretations, the effective pore space stiffness is unique. The porous glass data (open circles) are from a foam with approximately spherical pores. They fall along a trend, which at any porosity has a pore space stiffness that is roughly 50% stiffer than that of the high pressure sandstones (illustrating that even at high pressures, idealized spherical pores are poor representations of sandstone porosity). They also highlight the important result that constant pore *shape* is not equivalent to constant pore space *stiffness*. At each porosity, the pore shapes in the glass foam are nominally spheres; yet the pore space stiffness decreases by a factor of ~3 from $K_\phi/K_0 \approx 0.5$ at $\phi \approx 0.1$ to $K_\phi/K_0 \approx 0.16$ at $\phi \approx 0.5$. This illustrates the effect of elastic interaction: a pore sitting in the neighborhood of many other pores is effectively softer than the same pore sitting by itself (O'Connell and Budiansky, 1974). Finally, while these data are dynamic moduli determined from ultrasonic velocities, we expect that dry rock moduli measured at any frequency will have a similar interpretation. Winkler (1985, 1986) found, for example, that dry rocks generally have little or no velocity dispersion, at least relative to the large dispersion that occurs when pore liquids are introduced.

The high pressure sandstone and porous glass data in Figure 1 show fairly linear trends (Han, 1986; Nur, 1992), which can be approximated as

$$\frac{K_{dry}}{K_0} = 1 - \frac{\phi}{\phi_c}\left(1 - \frac{K_{dry}^{(R)}}{K_0}\right) \approx (1 - \phi/\phi_c), \qquad (7)$$

where the dry rock modulus K_{dry} approaches the effective mineral modulus K_0 at low porosity, and approaches the Reuss average (approximately zero in this case) as the porosity approaches some value, ϕ_c. Nur (1992) suggested that ϕ_c is the "critical porosity" that separates load-bearing sediments at lower porosities ($\phi < \phi_c$) from suspensions at higher porosities ($\phi > \phi_c$). He also noted that equation (7) can be interpreted as a "modified Voigt average" where the end members are no longer mineral (at $\phi = 0$) and air (at $\phi = 100\%$), but instead mineral (at $\phi = 0$) and the suspension (at $\phi = \phi_c$).

It is evident from the graph that any such straight line in the K_{dry} versus ϕ plane crosses contours of constant K_ϕ and therefore corresponds to progressively softer (more compressible) pore space with increasing porosity. In fact, from equation (1) it is easily shown that any straight line having the form of equation (7) must have a pore space stiffness that decreases linearly with porosity, in the form

$$K_\phi = K_0(\phi_c - \phi), \qquad (8)$$

where $K_\phi \approx \phi_c K_0$ at small porosity and $K_\phi \to 0$ as $\phi \to \phi_c$. We will show additional interpretations of the linear equations (7) and (8) in the following sections.

SATURATED ROCK COMPRESSIBILITY

The saturated rock compressibility β_{sat}, the reciprocal of the saturated rock bulk modulus K_{sat}, can be written in the form (see Appendix)

$$\frac{1}{K_{sat}} = \frac{1}{K_0} + \frac{\phi}{\tilde{K}_\phi}, \qquad (9)$$

where

$$\tilde{K}_\phi = K_\phi + \frac{K_0 K_f}{K_0 - K_f}. \qquad (10)$$

Here K_f is the pore fluid bulk modulus, and K_ϕ is the same dry pore-space stiffness defined in equation (2). This is a low-frequency result that assumes that any wave-induced increments of pore fluid pressure are uniform throughout the pore space. Note that the functional form of equation (9) for saturated rocks is exactly the same as equation (1) for dry rocks. The difference is only in the term $\tilde{K}_\phi$, defined in equation (10), which is equal to the dry pore stiffness K_ϕ, incremented by a fluid term $F = (K_0 K_f)/(K_0 - K_f)$.

Figure 2 shows a plot of normalized saturated rock bulk modulus, K_{sat}/K_0, versus porosity, computed from equation (9) for various values of $\tilde{K}_\phi/K_0$. (We actually plot K/K_0 versus porosity, where $K = K_{sat}$ for the saturated case.) Because equations (9) and (1) are alike, Figure 2 is exactly the same as Figure 1 except for the labeling ($\tilde{K}_\phi$ versus K_ϕ). In fact, Figure 2 and equation (9) can be used to describe dry rock moduli simply by noting that $\tilde{K}_\phi \to K_\phi$ as $K_f \to 0$. Hence, the vertical axis in Figure 2 should now be interpreted as the normalized *effective* bulk modulus K/K_0 where $K = K_{dry}$ for dry rocks and $K = K_{sat}$ for fluid-saturated rocks. "Fluid-saturated" now refers to any liquid or gas with arbitrary compressibility in the pores. Again, we caution that a gas at high pressures can have a nonnegligible bulk modulus.

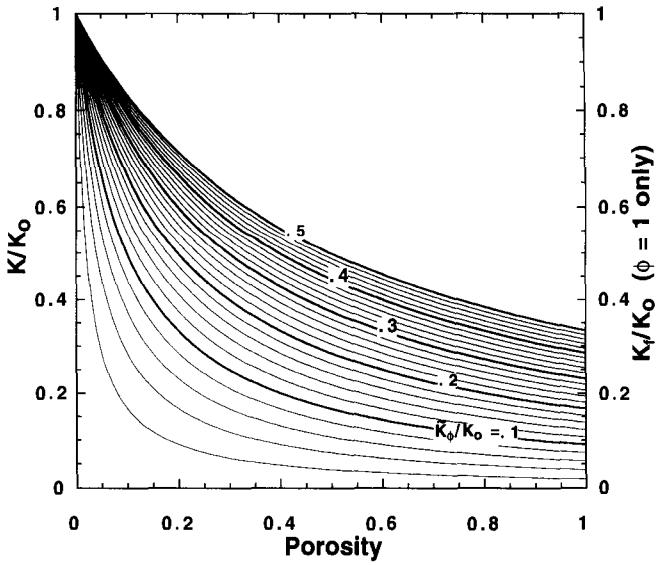

FIG. 2. Master curves of normalized rock effective bulk modulus versus porosity with contour of constant modified pore space stiffness. These curves apply to rocks with any mineral and any pore fluid. The effective bulk modulus K/K_0 should be interpreted as $K = K_{dry}$ for dry rocks and as $K = K_{sat}$ for fluid-saturated rocks. Note that the right vertical axis refers to values at the intercept $\phi = 1$ only, for the case when the contours are interpreted as the Reuss average.

Note that if $K_\phi \to 0$, then equation (9) reduces to the saturated rock Reuss average $K_{sat}^{(R)}$ of the fluid and mineral phases

$$\frac{1}{K_{sat}} \to \frac{1}{K_{sat}^{(R)}} = \frac{1-\phi}{K_0} + \frac{\phi}{K_f}. \tag{11}$$

Hence, each curve in Figure 2 can also be interpreted as the Reuss average modulus for a mixture of mineral and a fluid with bulk modulus K_f. The intercept of each curve with the right vertical axis is the corresponding fluid modulus K_f/K_0.

In summary, there are three different interpretations of the curves in Figure 2:

1) They show normalized *saturated* rock bulk modulus versus porosity for various values of modified pore stiffness $\tilde{K}_\phi$ for the general case when neither K_f nor K_ϕ is zero. (This is the most useful interpretation.)
2) They show normalized *dry* rock modulus versus porosity for various values of dry rock pore compressibility, if $K_f \to 0$. (In this case, $\tilde{K}_\phi$ is equal to K_ϕ.)
3) They show the *Reuss average* moduli versus porosity for various values of K_f. (In this case, $K_\phi = 0$.)

We found in the discussion of dry rock moduli that a linearly decreasing pore space stiffness having the form of equation (8) leads to a linear $K - \phi$ relation, having the form of equation (7), with a critical porosity ϕ_c. Since equation (9) has the same form as equation (1), it then follows that the corresponding saturated rock will also have a linear $K - \phi$ relation, with the same critical porosity

$$\frac{K_{sat}}{K_0} = 1 - \frac{\phi}{\phi_c}\left(1 - \frac{K_{sat}^{(R)}}{K_0}\right). \tag{12}$$

In other words, any straight lines drawn in the $K - \phi$ plane from $K/K_0 = 1$ and intersecting the Reuss average for that fluid at $\phi = \phi_c$ will transform under fluid substitution to another straight line intersecting the new Reuss average at the same critical porosity. We will use this property to demonstrate a simple graphical trick for applying the fluid transformation.

The property that a straight line in the $K - \phi$ plane maps to another straight line in the $K - \phi$ plane under a Gassmann transformation was shown, for example, in Nolen-Hoeksema (1993) and was labeled the modified Voigt average in Nur (1992). However, it is important to make the point that the straight lines themselves are not a consequence of Gassmann's equations. Gassmann's equation does not predict any particular $K - \phi$ relation.

THE FLUID SUBSTITUTION PROBLEM

One of the most important problems in the rock physics analysis of logs, cores, and seismic data is to predict seismic velocities in rocks saturated with one fluid from velocities in rocks saturated with a second fluid—or equivalently saturated rock velocities from dry rock velocities, and vice versa.

Generally, when a rock is loaded under an increment of compression, such as from a passing seismic wave, an increment of pore pressure change is induced which resists the compression and therefore stiffens the rock. The low-frequency Gassmann (1951)-Biot (1956) theory predicts the resulting increase in effective bulk modulus K_{sat} of the saturated rock as

$$\frac{K_{sat}}{K_0 - K_{sat}} = \frac{K_{dry}}{K_0 - K_{dry}} + \frac{K_f}{\phi(K_0 - K_f)}, \tag{13}$$

where ϕ is the porosity, and K_0, K_f, and K_{dry} are the bulk moduli of the mineral material, the pore fluid, and the dry rock, respectively. Gassmann predicted no change for the isotropic shear modulus with saturation, $\mu_{sat} = \mu_{dry}$. [Equation (13) can be derived from equation (9) by using equation (1) to eliminate the pore space compressibility.] Equation (13) assumes a homogeneous mineral modulus and statistical isotropy of the pore space but is free of assumptions about the pore geometry. Most importantly, it is valid only at sufficiently low frequencies such that the induced pore pressures are equilibrated throughout the pore space (i.e., that there is sufficient time for the pore fluid to flow and to eliminate wave-induced pore pressure gradients). This limitation to low frequencies explains why Gassmann's relation works best for very low-frequency in-situ seismic data (<100 Hz) and may not perform as well as frequencies increase toward sonic logging ($\sim 10^4$ Hz) and laboratory ultrasonic measurements ($\sim 10^6$ Hz) (Mavko and Jizba, 1991).

In practice, the fluid substitution is performed by first extracting the effective bulk and shear moduli from the measured velocities saturated with one pore fluid (or gas), transforming the bulk modulus to the new pore fluid using equation (13), and reconstructing the velocities corresponding to the change in modulus. Next we show two different methods for applying Gassmann's fluid substitution transform, equation (13), graphically.

Method 1: shift of $\tilde{K}_\phi$

The first method follows from noting in equation (10) that the only effect of a change in fluid is a change in the modified pore stiffness $\tilde{K}_\phi$. The method is applied by computing this change, $\Delta\tilde{K}_\phi$, and then jumping the appropriate number of contours. The procedure is as follows:

1) Plot the known effective modulus K corresponding to the rock saturated with fluid 1 (point A, in Figure 3) and identify the contour passing through it.
2) Compute the terms $F^{(1)} = (K_0 K_f^{(1)})/(K_0 - K_f^{(1)})$ for pore fluid 1 and $F^{(2)} = (K_0 K_f^{(2)})/(K_0 - K_f^{(2)})$ for the desired pore fluid 2.
3) From point A, move vertically (i.e., constant porosity) up or down the corresponding number of contours, $\Delta\tilde{K}_\phi = F^{(2)} - F^{(1)}$, and read off the new value of effective modulus K.

For the example shown, the starting point A was one of Han's (1986) data points, with effective dry rock bulk modulus $K_{dry}/K_0 = .44$, and porosity $\phi = .20$. Because it is dry, $F^{(1)}/K_0 \approx 0$. To saturate with water ($K_f/K_0 \approx 0.056$), we move up the amount $(F^{(2)} - F^{(1)})/K_0 = .06$, or three contours. The water-saturated modulus can be read off directly as $K_{sat}/K_0 = .52$, point A'. Obviously, the tech-

nique works equally well for going from dry to saturated, saturated to dry, or from one fluid to another. All we do is compute $\Delta F/K_0$ and count the contours.

The value of this method is to illustrate how the sensitivity of moduli (seismic velocities) to pore fluid changes is enhanced by high pore compressibility. Figure 3 shows a second data point (point B) which has the same porosity as the first example (point A), but a much lower dry rock bulk modulus (equivalently, a much smaller pore space stiffness, K_ϕ). The water saturated value, point B', is also shown. In both cases, the transfer from fluid 1 to fluid 2 (points A to A' and B to B') has the same change in the pore fluid term ΔF, and the same change in $\Delta\tilde{K}_\phi$, which translates into jumping three contours, anywhere on the plot. Yet, the resulting difference in effective rock modulus for point B is much larger than for point A. We get the well-known result that a rock with a large pore compressibility (i.e., a relatively low velocity for a given porosity) is more sensitive to pore fluid changes. Graphically, this is because the contours are farther apart at the bottom of the plot than at the top.

Method 2: Straight-line mapping

The second method also involves moving data points vertically, but the jump is constructed graphically with a straight edge. The method is based on a property that straight lines of the form of equation (7) remain straight lines under Gassmann's transformation.

The procedure is as follows:

1) Plot the known effective modulus K corresponding to the rock saturated with fluid 1 (point A, in Figure 4).
2) Define the Reuss averages for fluids 1 and 2 by identifying the contours that intersect the right vertical axis at $K_f^{(1)}/K_0$ and $K_f^{(2)}/K_0$.
3) Draw a straight line from $K/K_0 = 1$ through point A and mark the intersection with the Reuss average curve for fluid 1, which occurs at some porosity ϕ_c.
4) Move vertically up or down (at the same ϕ_c) to the Reuss average curve for fluid 2, and draw a straight line back to $K/K_0 = 1$.
5) The new data point A' lies on the new straight line, directly above A (at the same original porosity).

That the method is valid can be seen by substituting equation (7) into Gassmann's Equation (13).

This method is a rigorous, low-frequency version of Marion and Nur's (1991) bound averaging method (BAM). With BAM, it is assumed that the position of a data point relative to the upper and lower Hashin-Shtrikman (1963) bounds in the $K - \phi$ plane is a measure of pore space compressibility and is therefore the same for any fluid. To make the BAM estimate, the fractional position of the data point is measured relative to bounds computed for the starting fluid. Then, the bounds are recomputed with the new fluid, and the new modulus is read relative to them. BAM appears to give reasonable estimates of the moduli under fluid substitution but is strictly a heuristic approach. Our graphical method uses a slightly different rescaling of the data relative to the Reuss bound (identical to the lower Hashin-Shtrikman bound, in this case) and implements Gassmann's relations exactly.

Another important point that this method highlights is that an unconsolidated rock that has essentially zero moduli

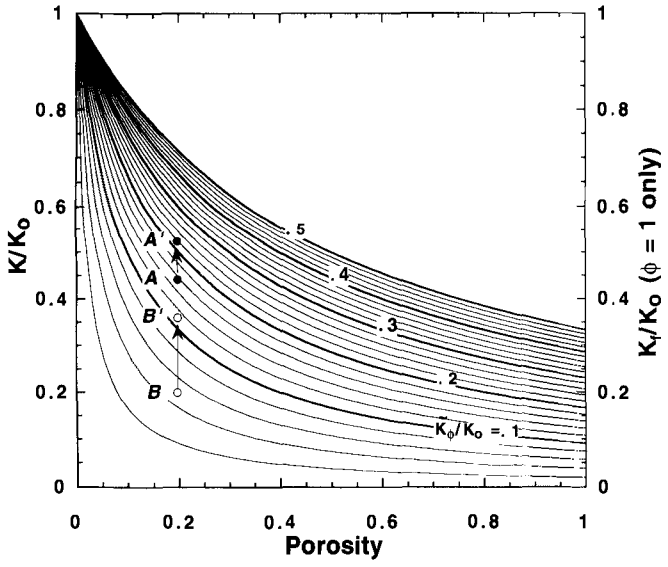

FIG. 3. Fluid substitution in terms of pore stiffness. Points A and B are dry rock values; A' and B' are the corresponding values saturated with water. When expressed in terms of the modified pore stiffness, Gassmann's (1951) equation is applied by simply jumping a fixed number (that depends on the fluids) of contours. This illustrates that a rock with a large pore compressibility (i.e., a relatively low velocity for a given porosity) is more sensitive to pore fluid changes.

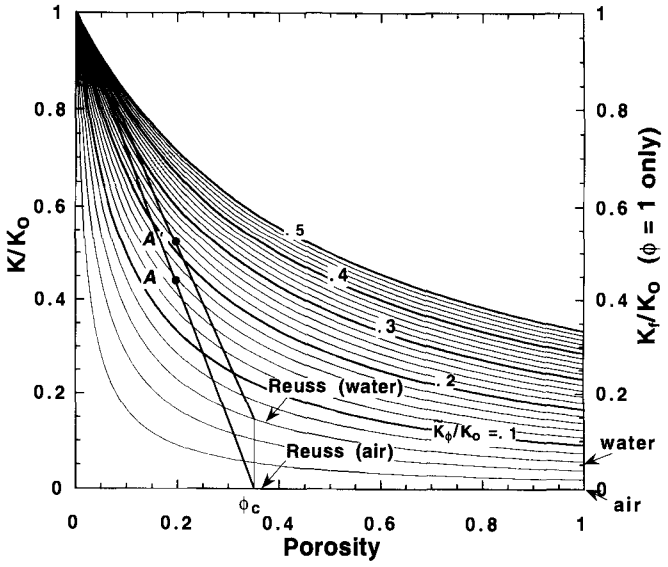

FIG. 4. Graphical construction for applying Gassmann's (1951) equation. For a given rock with any pore fluid, a straight line drawn from the mineral modulus (on the vertical axis) through the data point, will always intersect the Reuss average at the same porosity, which is a property of the rock sample. A change of fluid corresponds then to simply finding the Reuss curve that intersects the right vertical axis with the fluid's modulus.

when dry (i.e., its moduli fall on the dry Reuss average) must remain on the Reuss average when saturated with a fluid.

CONCLUSIONS

The pore space compressibility of rocks is related in a simple way to effective bulk modulus, which is directly related to measurable seismic velocities. The pore compressibility is also the direct physical link between the dry and fluid-saturated moduli and is therefore the basis of Gassmann's equation for fluid substitution. For a fixed porosity, an increase in pore space compressibility increases the sensitivity of the modulus to fluid substitution. Therefore, geophysical monitoring of reservoir changes caused by the production or EOR processes will generally be most effective in high compressibility reservoirs. Finally, we have shown how these simple relations can be interpreted graphically in terms of the pore compressibility. The change of effective bulk modulus caused by a change in pore fluids [Gassmann's (1951) fluid substitution problem] can be estimated (1) by simply jumping a fixed number (that depends on the fluids) of pore stiffness contours on the modulus-versus-porosity plot, or (2) by a straight line construction that rescales the moduli using the Reuss average.

ACKNOWLEDGMENTS

This work was supported by the Stanford Rock Physics and Borehole Geophysics Project, Gas Research Institute contract 5093-260-2703, and EPA contract R 819885-01-0. Thanks to Profs. Wayne Pennington and Guy Towle for many useful comments.

REFERENCES

Biot, M. A., 1956, Theory of propagation of elastic waves in a fluid saturated porous solid. I. Low-frequency range: J. Acoust. Soc. Amer., **28**, 168–178.

Bredehoeft, J. D., and Hanshaw, B. B., 1968, On the maintenance of anomalous fluid pressures I, thick sedimentary sequences: Geol. Soc. Am. Bull., **79**, 1097–1106.

Eshelby, J. D., 1957, The determination of the elastic field of an ellipsoidal inclusion, and related problems: Proc. Roy. Soc., **A241**, 376–396.

Gassmann, F., 1951, Uber die elastizitat poroser medien: Vier. der Natur Gesellschaft, **96**, 1–23.

Han, D., 1986, Effects of porosity and clay content on acoustic properties of sandstones and unconsolidated sediments: Ph.D. dissertation, Stanford University.

Hashin, Z., and Shtrikman, S., 1963, A variational approach to the elastic behavior of multiphase materials: J. Mech. Phys. Solids, **11**, 127–140.

Jaeger, J. C., and Cook, N. G. W., 1969, Fundamentals of rock mechanics: Chapman and Hall.

Jizba, D., 1991, Mechanical and acoustical properties of sandstones and shales: Ph.D. dissertation, Stanford University.

Kuster, G. T., and Toksöz, M. N., 1974, Velocity and attenuation in two-phase media: Part II experimental results: Geophysics, **39**, 587–606.

Marion, D., and Nur, A., 1991, Pore-filling material and its effect on velocity in rocks: Geophysics, **56**, 225–230.

Mavko, G., and Jizba, D., 1991, Estimating grain-scale fluid effects on velocity dispersion in rocks: Geophysics, **56**, 1940–1949.

Mavko, G., and Nur, A., 1978, The effect of nonelliptical cracks on the compressibility of rocks: J. Geophys. Res., **83**, 4459–4468.

Murphy, W., Reischer, A., and Hsu, K., 1993, Modulus decomposition of compressional and shear velocities in sandstones: Geophysics, **58**, 227–239.

Nolen-Hoeksema, R. C., 1993, Porosity and consolidation limits of sediments and Gassmann's elastic-wave equation: Geophys. Res. Lett., **20**, 847–850.

Nur, A., 1989, Four dimensional seismology and (true) direct detection of hydrocarbons: the petrophysical basis, Geophysics: The Leading Edge, **8**, No. 9, 30–36.

——— 1992, Critical porosity and the seismic velocities in rocks: EOS, Transactions Am. Geophys. Union, **73**, 43, 66.

O'Connell, R., and Budiansky, B., 1974, Seismic velocities in dry and saturated cracked solids: J. Geophys. Res., **82**, 5719–5736.

Reuss, A., 1929, Berechnung der fliessgrense von mishkristallen: Zeitschrift fur Angewandte Mathematik und Mechanik, **9**, 49–58.

Voigt, W., 1928, Lehrbuck der Kristallphysik: Teubner, Leipzig.

Walsh, J., 1965, The effect of cracks on the compressibility of rock: J. Geophys. Res., **70**, 381–389.

Walsh, J. B., Brace, W. F., and England, A. W., 1965, Effect of porosity on compressibility of glass: J. Amer. Cer. Soc., **48**, 605–608.

Winkler, K. W., 1985, Dispersion analysis of velocity and attenuation in Berea sandstone: J. Geophys. Res., **90**, 6793–6800.

——— 1986, Dispersion analysis of velocity and attenuation in Berea sandstone: Geophysics, **56**, 1331–1348.

Zimmerman, R. W., 1991, Compressibility of Sandstones: Elsevier Science Publ.

APPENDIX

DERIVATION OF PORE FLUID AND PORE COMPRESSIBILITY EFFECTS

The dry and saturated bulk moduli are estimated using the Betti-Rayleigh reciprocity theorem (Walsh, 1965; Jaeger and Cook, 1969). The theorem states that for a given linear elastic body acted upon by two different sets of forces, the work done by the first set of forces acting through the displacements caused by the second set of forces is equal to the work done by the second set of forces acting through the displacements caused by the first set of forces.

Consider experiments A, B, and C applied to a rock with total volume V and pore volume v_p as shown in Figure A-1. Experiment A has uniform hydrostatic stress $\Delta\sigma$ applied to all surfaces inside and outside the rock. In this case it is easy to show that the rock deforms like a solid block without pores. In particular, the fractional volume change of the entire sample, or of any particular pore, can be written as

$$\frac{\Delta v}{v} = \frac{\Delta\sigma}{K_0}, \tag{A-1}$$

where v is any volume of interest. Experiment B has the same hydrostatic stress $\Delta\sigma$ applied only to the outside surfaces of the rock. The pore surfaces are stress free. In this case, the outside surfaces of the sample deform with the effective dry rock bulk modulus K_{dry}, which we are seeking. Experiment C has the hydrostatic stress $\Delta\sigma$ applied to the outside surfaces of the sample, while the induced pore pressure increment ΔP of the saturated rock is applied to the pore surfaces. In this case, the outside surfaces deform with the effective saturated rock bulk modulus K_{sat}, which we are also seeking. In all of our derivations, we define both confining stress $\Delta\sigma$ and pore pressure ΔP to be positive in tension.

Applying the theorem to experiments A and B, we can write

$$\Delta\sigma\ \Delta V_{dry} - \Delta\sigma\ \Delta v_p = \Delta\sigma\ \Delta V_0, \tag{A-2}$$

where ΔV_{dry} is the total volume change of the external surfaces and Δv_p is the pore volume change, both in the dry rock experiment B; and ΔV_0 is the total sample volume change in experiment A. Then noting that $\Delta V_{dry} = \Delta\sigma V/K_{dry}$ and $\Delta V_0 = \Delta\sigma\ V/K_0$, we can write

$$\Delta\sigma\ \frac{\Delta\sigma}{K_{dry}}\ V - \Delta\sigma\ \Delta v_p = \Delta\sigma\ \frac{\Delta\sigma}{K_0}\ V. \tag{A-3}$$

Dividing through by $\Delta\sigma^2 V$ gives

$$\frac{1}{K_{dry}} - \frac{1}{V}\frac{\Delta v_p}{\Delta\sigma} = \frac{1}{K_0}. \tag{A-4}$$

Finally noting that $\phi = v_p/V$ and taking the limit as $\Delta\sigma \to 0$ gives Equation (1).

Applying the theorem to experiments A and C, we can write

$$\Delta\sigma\ \Delta V_{sat} - \Delta\sigma\ \Delta v_{p-sat} = \Delta\sigma\ \Delta V_0 - \Delta P\ \Delta v_{p0}, \tag{A-5}$$

where ΔV_{sat} is the total volume change of the external surfaces and Δv_{p-sat} is the pore volume change, both in the saturated rock experiment C, and ΔV_0 is the total sample volume change and Δv_{p0} is the pore volume change, both in experiment A. Then noting that $\Delta V_{sat} = \Delta\sigma\ V/K_{sat}$, $\Delta V_0 = \Delta\sigma\ V/K_0$, and $\Delta v_{p0} = \Delta\sigma\ v_p/K_0$ we can write

$$\Delta\sigma\ \frac{\Delta\sigma}{K_{sat}}\ V - \Delta\sigma\ \Delta v_{p-sat} = \Delta\sigma\ \frac{\Delta\sigma}{K_0}\ V - \Delta P\ \frac{\Delta\sigma}{K_0}\ v_p. \tag{A-6}$$

The saturated pore volume change can be related to the pore pressure increment using the fluid bulk modulus

$$\frac{\Delta v_{p-sat}}{v_p} = \frac{\Delta P}{K_f}. \tag{A-7}$$

The pore pressure increment induced by the applied hydrostatic stress can be written in terms of the fluid modulus and dry pore space stiffness as

$$\frac{\Delta P}{\Delta\sigma} = \frac{1/K_0}{\dfrac{1}{K_\phi} + \dfrac{1}{K_f} - \dfrac{1}{K_\phi}}. \tag{A-8}$$

Finally, combining equations (A-6)–(A-8) gives equation (9).

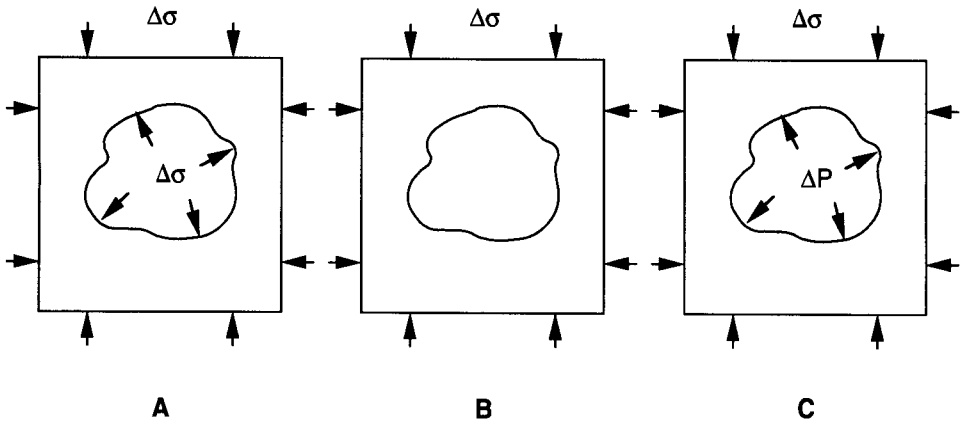

FIG. A-1. Applying the reciprocity theory to three different stress states. On the left, the same tractions are applied to the inside and outside surfaces, so the rock deforms with the mineral modulus. In the middle, the same tractions are applied to the outside surface, but the inside surfaces are traction-free, so the rock deforms with the dry rock modulus. On the right, the same tractions are applied to the outside surfaces, with the as-yet unknown induced pore pressure applied to the inside surfaces, so the sample deforms with the saturated rock modulus.